Biomimetic Model of Articular Cartilage Based on In Vitro Experiments

Patrick A. Smyth[1,a], Itzhak Green[1,b], Robert L. Jackson[2,c], R. Reid Hanson[3,d]

[1]Department of Mechanical Engineering, Georgia Institute of Technology, USA, Atlanta, Georgia 30332

[2]Department of Mechanical Engineering, Auburn University, USA, Auburn, Alabama 36849

[3]College of Veterinary Medicine, Auburn University, USA, Auburn, Alabama 36849

[a]pasmyth4@gatech.edu, [b]itzhak.green@me.gatech.edu, [c]jacksr7@auburn.edu, [d]hansorr@auburn.edu

Abstract. Articular cartilage is a complicated material to model for a variety of reasons: its biphasic/triphasic properties, heterogeneous structure, compressibility, unique geometry, and variance between samples. However, the applications for a biomimetic, cartilage-like material are numerous and include: porous bearings, viscous dampers, robotic linkages, artificial joints, etc. This work reports experimental results on the stress-relaxation of equine articular cartilage in unconfined compression. The response is consistent with simple spring and damper systems, and gives a storage and loss moduli. This model is proposed for use in evaluating biomimetic materials, and can be incorporated into large-scale dynamic analyses to account for motion or impact. The proposed characterization is suited for high-level analysis of multi-phase materials, where separating the contribution of each phase is not desired.

Introduction

Healthy cartilage provides compressive load support and facilitates near frictionless motion within articulating joints. This flexible substance allows for motion within the joint while protecting the bone ends from grinding and wear. When this protection fails, osteoarthritis occurs. To understand healthy and damaged cartilage for biomimetic applications, mechanical tests are performed. In stress-relaxation experiments on healthy cartilage extracted from equine joints, elastic and dissipative mechanisms are displayed. Understanding these mechanisms can lead to advances in other fields, such as flexible bearings in rotordynamic systems [1, 2], or improved porous bearings in industrial applications [3].

The majority of cartilage research has focused on the interactions of the collagen matrix and the lubricating synovial fluid that permeates the joint capsule [4, 5, 6, 7, 8]. In addition, many attempts have been made to develop constitutive relations for cartilage. The prevailing theories account for the biphasic (solid-fluid) and triphasic (solid-fluid-ionic) properties of cartilage [9, 10, 11, 12]. While this is a physiologically comprehensive model that separates the two (or three) phases of cartilage, the models do not typically match experimental results well. An alternative way of modeling cartilage is to consider the solid and fluid interactions as part of a total mechanical response. The goal is to describe the conglomerate behavior of cartilage. This is useful for biomimetics, where a simple, descriptive model is required. A phenomenological approach, post hoc of experimentation, can provide such a model. Mechanical systems are well-suited for this application because they include a mechanism for energy storage and dissipation. The dissipation comes from frictional drag between the solid and fluid phases, compressibility of the solid matrix, or other mechanisms. The use of fewer material parameters allows for an extremely convenient comparison of engineered substances. The analogy to mechanical systems is deliberate for incorporation in engineering designs. Such a model will be useful in the design and construction of biomimetic materials (e.g. hard and soft foams, gels, and various two-phase combinations). For additional information on cartilage modeling, the reader is referred to Mow and others [13, 14].

Spring and damper models are not new to cartilage mechanics, but most studies limit their use to the solid part of a biphasic response. However, experimental work shows that these simple mechanical systems capture a large range of cartilage behavior. While the biphasic and triphasic theories remain popular among researchers, a phenomenological model for two-phase materials has utility in biomimetics. The experimental results indicate that viscoelasticity is appropriate for considering the conglomerate behavior of cartilage.

In the 1970's, Coletti et al. [15] and Parsons and Black [16] used spring and damper models to characterize cartilage. Creep tests were performed on cartilage samples with limited success in matching the models to the experimental results. Coletti et al. determined that cartilage exhibits non-linear viscoelastic behavior dependent on strain. While some attempts were made to model cartilage phenomenologically, the majority of research was focused on constitutively modeling the separate phases of cartilage. This was the genesis of the biphasic theory [9, 10, 11, 12, 17].

At the same time as the biphasic model was being developed in 1980, Woo et al. [18] looked at cartilage samples in tension, performing stress-relaxation experiments. Fung's model [19] for soft tissue is utilized in the work. The experiments compare favorably to the compression relaxation experiments of Mow and others [20]; however, the experimental setup prevented the tests from being ``true" relaxation tests. Extending the model proposed by Fung, Simon et al. [21] performed relaxation experiments on cartilage specimens. The biphasic and solid models are compared. Simon's work shows the advantage of mechanical models in that they look at the macro-scale response of cartilage. However, this is a disadvantage if it is desired to separate the contributions of the solid and fluid phases.

More recently, Wang [22], Ehlers and Markert [23, 24] and Wilson et al. [25, 26] have used various spring and damper representations to model the fibril part of cartilage. The poroviscoelastic fibril reinforced model developed by Wilson et al. considers the local morphology of collagen fibers and their apparent strong influence on stress and strain (the springs are strain-dependent, or non-linear). Wilson's work compares favorably to DiSilvestro and Suh's [27]. Garcia et al. [28] uses a similar model to Wilson's [25, 26] to describe the solid portion of the nonlinear biphasic model. Finally, Julkunen et al. [29] corroborates the work of Wilson et al. [25, 26] with a FEM study, finding good agreement between the experiment and model in stress-relaxation applications.

Using spring and dashpot systems to model cartilage is not new, and certainly the use of stress-relaxation experiments is well-established. However, as discussed by Argatov [30] there is a need for a simple, but complete, model for cartilage. The utility of such a model is apparent in larger scale studies, e.g. when cartilage is incorporated into an impact study. Here, a phenomenological model is better suited for the analysis because the cost of including a complex model is not worth the additional fidelity (if there is any). Argatov notes that the viscoelastic models are not ``true" mathematical descriptions of cartilage; however, the behavioral characteristics are widely applicable. This concept can be extended to other two-phase materials as well, where the spring and damper systems allow for efficient modeling. In particular, the proposed model would be appropriate for biomimetic applications such as biphasic dampers.

Multiple experimental procedures exist for cartilage. Those used by [9, 31, 32] remain the predominate means for testing cartilage today. Figure 1(a) shows how the pseudo-relaxation experiment is performed in a confined compression. In these tests, the fluid is forced in the vertical direction through a porous indenter. The tests require a ramp displacement loading (approximately 2 seconds or greater) to allow fluid to permeate the indenter or punch (Fig. 1(b)). The ramp input is not analogous to the type of motion experienced during walking or running. A ``true" stress-relaxation experiment cannot be performed in confined compression, as the confining chamber creates super high stresses (hydrostatic pressure) in the cartilage plugs when an instantaneous displacement is attempted. Additionally, the confining chamber creates a 3D stress field on the cartilage plug throughout. This is because the cartilage is restrained by the rigid walls of the chamber. For example, consider an isotropic, elastic material- the stress and strain relations are determined as follows in cylindrical coordinates [33]:
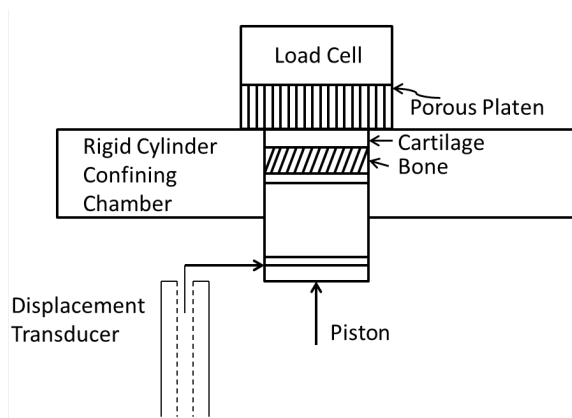
(a) Reproduction of test setup from [9, 31, 32]
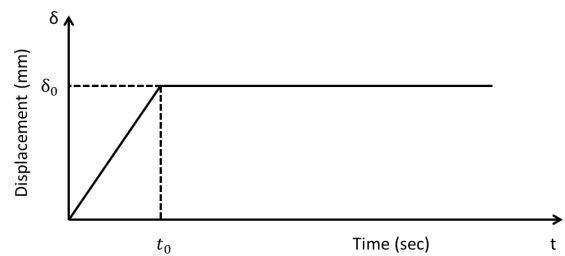
(b) Reproduction of ramp input from [9, 31, 32]
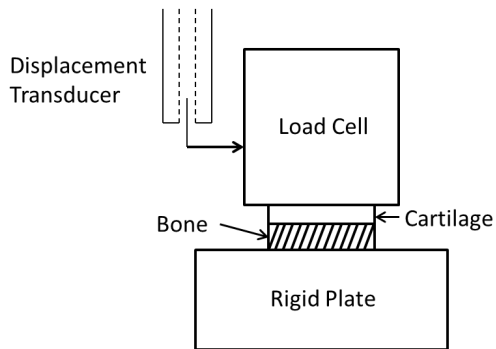
(c) Schematic of test setup in current study

(d) Instantaneous displacement used in current study

Fig. 1: Comparison of experimental setups for measuring cartilage

$$\begin{Bmatrix} \sigma_r \\ \sigma_\theta \\ \sigma_z \end{Bmatrix} = \frac{E}{(1+\nu)(1-2\nu)} \begin{bmatrix} 1-\nu & \nu & \nu \\ \nu & 1-\nu & \nu \\ \nu & \nu & 1-\nu \end{bmatrix} \begin{Bmatrix} \epsilon_r \\ \epsilon_\theta \\ \epsilon_z \end{Bmatrix} \tag{1}$$

or for strain in terms of stress:

$$\{\epsilon\} = \begin{Bmatrix} \epsilon_r \\ \epsilon_\theta \\ \epsilon_z \end{Bmatrix} = \frac{1}{E} \begin{bmatrix} 1 & -\nu & -\nu \\ -\nu & 1 & -\nu \\ -\nu & -\nu & 1 \end{bmatrix} \begin{Bmatrix} \sigma_r \\ \sigma_\theta \\ \sigma_z \end{Bmatrix} \tag{2}$$

According to Eq. 1, Poisson's ratio is needed in the confined compression case ($\epsilon_r = \epsilon_\theta = 0$) to obtain stress in the z (vertical) direction:

$$\sigma_z = \left[\frac{E(1-\nu)}{(1+\nu)(1-2\nu)} \right] \epsilon_z. \tag{3}$$

Poisson's ratio must be assumed or determined experimentally, which adds an additional parameter to the models using confined compression experiments. It is likely that Poisson's ratio is also time or frequency dependent; therefore, it poses another challenge to determine. Poisson's ratio is *not* needed for the uniaxial, unconfined compression case ($\sigma_r = \sigma_\theta = 0$) because stress and strain are related only by E (see Eq. 2):

$$\sigma_z = E\epsilon_z. \tag{4}$$

The unconfined case shown in Fig. 1(c) does not suffer from the limitations of confined compression. Therefore, a practically instantaneous displacement can be physically imposed on the cartilage sample, as shown in Fig. 1(d). This mimics a classical relaxation case to a step strain. Precisely such a test is needed to directly extract the storage and loss moduli. For a stress-relaxation test, unconfined compression offers multiple advantages over the confined compression used in prior studies [9, 31, 32]. Unconfined compression experiments are used in the current study in part because Poisson's ratio is difficult to determine for a multi-phasic substance such as cartilage. Although the fluid flows in a different direction in unconfined compression, a material property must be an invariant property regardless of the test performed; or conversely if a property depends on the test performed, it cannot be considered a material property.

Materials and Methods

Articular cartilage samples are harvested from the right stifle joints of horses that are euthanized for other reasons. Equine samples are used for multiple reasons: the cartilage surfaces are large and allow for ``macro-scale" analysis, the joints carry large loads (meaning that there are typically higher stresses within the joints), and the availability of samples is suitable. In addition, equine and human articular cartilage have similar structural features and collagen organization [34].

After euthanasia, intact joints are removed from the horses. The joints remain sealed in their native joint capsule until they are needed for analysis. The cartilage is harvested by dissection of the surrounding tissue, and resized with an industrial bandsaw. The cartilage surface is hydrated with a saline solution (0.9%) to prevent drying.

The medial condyle of the right rear stifle is used for study. The stifle joint is mechanically analogous to the human knee, and the condyle contains an area of thick and relatively flat cartilage. It is

(a) Side schematic of stifle joint before plug is created

(b) Punch embedded in the cartilage as the surrounding structure is removed

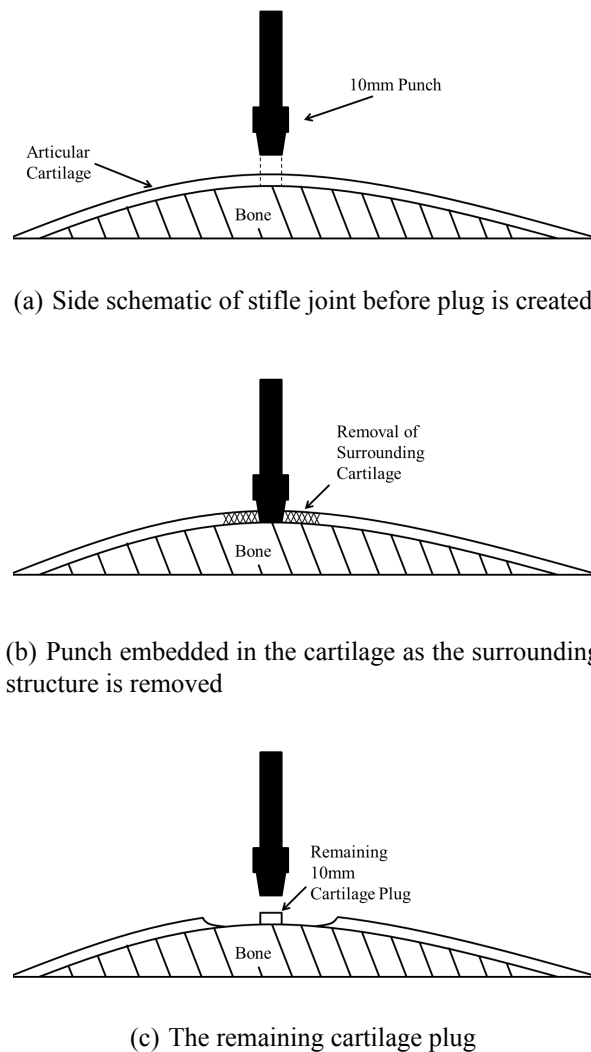
(c) The remaining cartilage plug

Fig. 2: Schematic of the 10 mm plug creation process

hoped that the equine results can eventually be extrapolated to human studies, where artificial knee replacements are the second most common type of surgical replacement, behind hip joint replacements.

After bulk harvesting and resizing of the condyle, a 10 mm plug is created with a hollow punch. The punch is driven into the sample with an arbor press, depicted in Fig. 2. With the punch embedded in the cartilage and subchrondial bone, the surrounding cartilage is removed with a rotary device. The punch has an access hole to allow for hydration of the sample. After the plug is created, it is immersed in a biological medium. The average time from the beginning of dissection to immersion is less than 20 minutes. The joint capsule is open for approximately 10 minutes during the process.

The cartilage plugs are placed in a UMT CETR tribometer. The tribometer imposes a nearly instantaneous (within approximately 30 ms) displacement on the cartilage surface, while tracking the force generated in the cartilage matrix. By design, this is a stress-relaxation experiment. The tribometer holds a 12 mm rigid aluminum cylinder attached to a load cell, as shown in Fig. 3. Initially, the cylinder contacts the cartilage surface with a preload of 0.5 N. The preload ensures that the cylinder makes complete contact with the cartilage surface. In effect, the cylinder is flattening out any curvature in the cartilage. At time $t = t_0$, a downward displacement is imposed on the cartilage and the resulting force is measured. After approximately 180 seconds of measurement, the rigid cylinder is withdrawn from the surface. The cartilage is allowed two minutes to recover between tests, and the procedure is repeated. Testing indicated that the recovery time was sufficient (additional time did not change the results). The typical test includes four runs at a lower strain, followed by four runs at a higher strain.
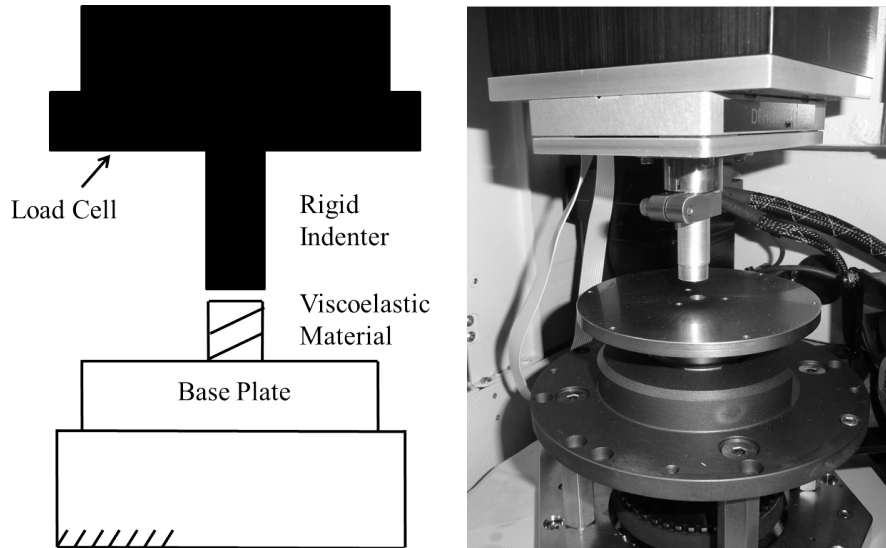
Fig. 3: CETR UMT3 Tribometer fitted with a 12 mm rigid indenter

Typically, displacements of 0.25 mm and 0.35 mm are imposed on the cartilage matrix. The cartilage thickness is measured after the relaxation experiment, so *a priori* strains can not be determined. However, the displacements are designed to strain the cartilage matrix from 5-15%. The relaxation behavior usually reaches an equilibrium by the test's conclusion. In all cases, the bulk of the relaxation behavior has occurred by 180 seconds, and the steady-state (rubbery modulus) information can be extrapolated with the proposed model.

Needle probe techniques are used to determine the thickness of the cartilage plugs. The measurements are averaged to produce a mean thickness. The thickness is needed to determine the modulus.

The stress-relaxation experiment is particularly useful as a biomimetic model because it contains a wide spectrum of storage and loss properties. In 1962, Gurtin and Sternberg [35] developed a constitutive law relating stress, strain and the relaxation modulus using Boltzmann's superposition principle. The viscoelastic model is time-dependent, or in other words, it retains memory of the material history:

$$\sigma\left(t\right) = \epsilon\left(0\right) E\left(t\right) + \int_{0}^{t} \dot{\epsilon}\left(\tau\right) E\left(t - \tau\right) \, \mathrm{d}\tau. \tag{5}$$

where $\sigma\left(t\right)$ is the stress, $\epsilon\left(t\right)$ is the strain, and $E\left(t\right)$ is the relaxation modulus. Typically, $\sigma(t)$ and $\epsilon(t)$ are either set or measured during experimentation, while $E\left(t\right)$ is obtained from a fixed strain input $\epsilon = \epsilon_{step}$, such that $E(t) = \sigma(t)/\epsilon_{step}$. The parameters of stress, strain, and elastic modulus in Eq. 5 are time-dependent. It should be noted that Eq. 5 describes a linear relationship between the strain history and the current stress. Transferring Eq. 5 into the Laplace domain allows for simple treatment of the convolution integral:

$$\sigma\left(s\right) = sE\left(s\right)\epsilon\left(s\right) \tag{6}$$

Equation 6 is similar to Hooke's Law in the Laplace domain (for the uniaxial case). This provides the foundation for the elastic-viscoelastic correspondence principle.

To transfer between the Laplace and frequency domains, the s in Eq. 6 is replaced with $i\omega$, where i is defined as $\sqrt{-1}$ and ω is the frequency in rad/s.

Hence, applying $s \to i\omega$, Eq. 6 becomes:

$$\sigma(\omega) = (i\omega) E(\omega) \epsilon(\omega) \triangleq E^*(\omega)\epsilon(\omega) \tag{7}$$

where:

$$E^* = (i\omega) E(\omega) \tag{8}$$

E^* is the complex modulus, which has two components- a real and an imaginary:

$$E^*(\omega) = E'(\omega) + iE''(\omega) \tag{9}$$

The real component (E') is known as the storage modulus, while the imaginary component (E'') is known as the loss modulus. Both measures describe the dynamic behavior (frequency dependency) of the material. The correspondence principle is powerful because one constitutive formulation determines the amount of modulus retained (stored) or lost (loss). Accurate stress-strain constitutive equations must be formed to describe cartilage or a biomimetic material.

Spring and dashpot systems have both elastic and dissipative mechanisms simultaneously [35, 36, 37]. The dissipative mechanisms are rate-dependent, much like a dashpot or damper in physical systems. The Prony series (Fig. 4) is one such model. The Prony series model is composed of a free spring and an infinite series of Maxwell elements in parallel. Each Maxwell element is an individual spring and dashpot in series.
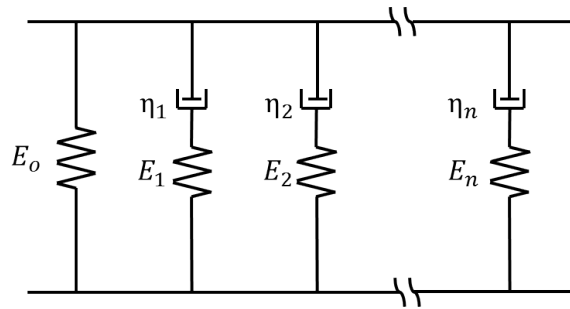

Fig. 4: Prony series

The Prony series captures the a wide spectrum of behavior- at high frequencies the dashpots ``lock,'' and become rigid. Here, only the springs contribute to the mechanical response. At low frequencies, the individual Maxwell elements have no contribution to the overall load support (the dashpots in the Maxwell elements transmit a negligible force). Therefore, the only load support comes from the free spring, E_0. This model accurately captures features that are seen in cartilage and biomimetic materials.

The functional form of the Prony series combines multiple exponentially decaying functions:

$$\sigma_T = \left(E_0 + \sum_{n=1}^{\infty} E_n e^{\lambda_n t} \right) \epsilon_0, \tag{10}$$

which mimics the stress-relaxation behavior seen in cartilage. The infinite sum in Eq. 10 allows for different decades of relaxation. For instance, a material that rapidly expels energy may require many short-lived decay terms, which the Prony model accommodates easily. Although the Prony series is a robust model, it may require a large number of Maxwell elements to fully capture material behavior. The additional terms in the Prony series expand the eigenvalue problem, and make extrapolation more

difficult. The Prony model readily characterizes the stress-relaxation behavior of biphasic materials like cartilage.

The Prony series is fit in the time-domain. At a given strain, some stiffening occurred between experiments; therefore, the model was fit to the average relaxation data. The experimental data is particularly noisy from the tribometer. Transferring the raw experimental signal from the time to the frequency domain is challenging, even with filtering and smoothing algorithms. Therefore, the analytic form of the Prony series in the frequency domain is used:

$$E(\omega) = \frac{E_0}{i\omega} + \sum_{n=1}^{\infty} E_n \left(\frac{\lambda_n - i\omega}{\lambda_n^2 + \omega^2} \right) \tag{11}$$

The storage and loss moduli are given as a function of frequency, ω, respectively:

$$E' = E_0 + \sum_{n=1}^{\infty} \omega^2 \left(\frac{E_n}{\lambda_n^2 + \omega^2} \right) \tag{12}$$

$$E'' = \sum_{n=1}^{\infty} \left(\frac{E_n \lambda_n \omega}{\lambda_n^2 + \omega^2} \right) \tag{13}$$

The parameters λ_n and E_n are obtained from the time-domain fit.

The tribometer samples at 1000 Hz, which yields approximately 180,000 data points for a typical experiment. A least squares fitting routine is implemented in Matlab to parse the combined relaxation data. For a full dynamic simulation, the eigenvalue problem is minimized by fitting the relaxation data with as few terms as possible. However, more terms typically describe material behavior better. The consequence of increasing the number of terms is that the model develops ``wiggles" in the frequency domain. These wiggles are not material based, but rather a figment of the modeling. In this regard, the fewer Prony terms that can be used, the better. The fitting routine also begins to fail to converge when the number of Prony terms gets too high ($n \geq 5$). The convergence issues are due to the least squares algorithm becoming ill-conditioned. When this occurs, the Prony terms are more difficult to uniquely define. Four Prony terms is the maximum that can be fit reliably to the experimental data; however, this covers a wide spectrum of cartilage and biomimetic material behavior.

Results

A four-term Prony series is used to fit the relaxation behavior, which is pronounced in the initial seconds of the experiment (Fig. 5(a)). In general, the four-term Prony series does a suitable job fitting the relaxation behavior. In the initial decay period (1s), some deviation between the fit and the actual data is seen. The deviation between the model and experimental data corresponds to the highest frequency information. For horses (and humans), frequency ranges greater than 5 Hz are not accessed during even the most strenuous exercises. Therefore, it is less important to accurately capture this region of the relaxation. The physiological region of the relaxation occurs from $t = 0.25s$ and on. The Prony series is able to robustly model these decades of relaxation behavior (shown in Fig. 5(b) using a semi-log scale), which makes its utility apparent.

The empirical data indicates that the decay properties of cartilage are strain-dependent. Cartilage exhibits greater stiffness with higher strain, and appears to decay more slowly. An effective time constant is created to quantify this observation. In exponential decay, the time constant represents the time it takes for the response to reach $\left(\frac{1}{e} \right)$ of the initial value. This is typical of a first-order system that mimics the relaxation behavior. For a series of exponential decays, the effective time constant can
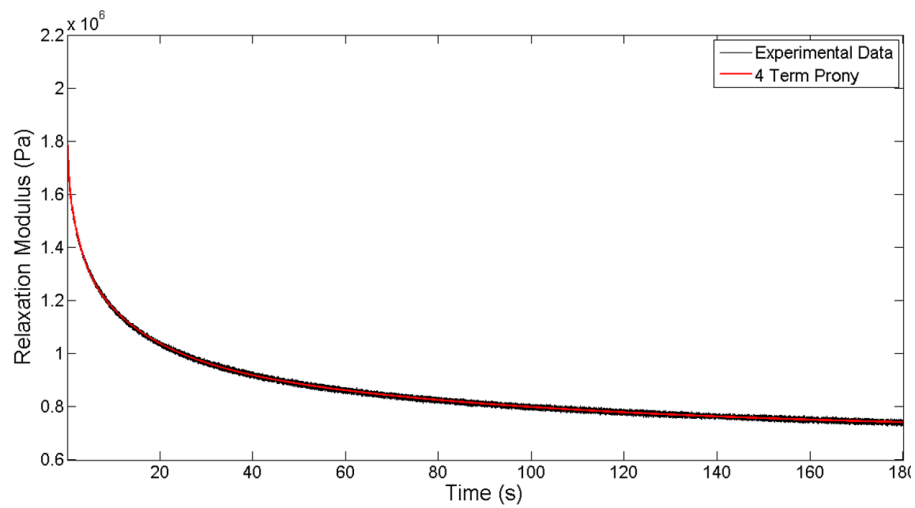
(a) Example of a four-term Prony fit to experimental data (Saline (d))
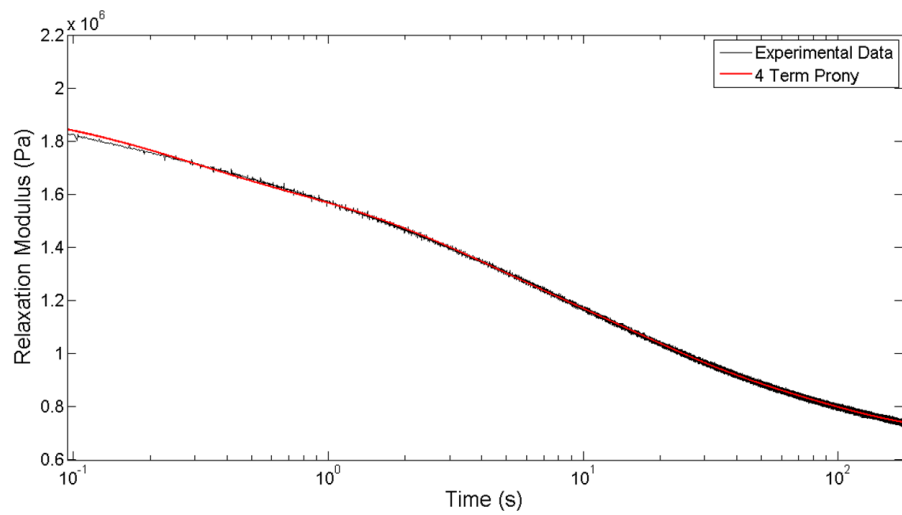
(b) Four-term Prony series fit, displayed on a semi-log scale (Saline (d))

Fig. 5: Example fit of Prony Series (Saline (d))

Table 1: Time constant information for cases immersed in saline

Name	Lower Strain (s)	Higher Strain (s)
Saline (a)	1.57	1.98
Saline (b)	6.38	8.36
Saline (c)	5.00	10.06
Saline (d)	10.28	15.36
Saline (e)	17.06	13.23
Saline (f)	15.71	19.37

be found by locating the time when 63.2% of the relaxation has occurred. This means $0.368 = 36.8\%$ of $E(t)$ remains. The time constant is found numerically with Matlab. The flowchart shown in Fig. 6 outlines the process taken to locate the time constant. When the relaxation threshold is reached, the program records the time and exits the loop.
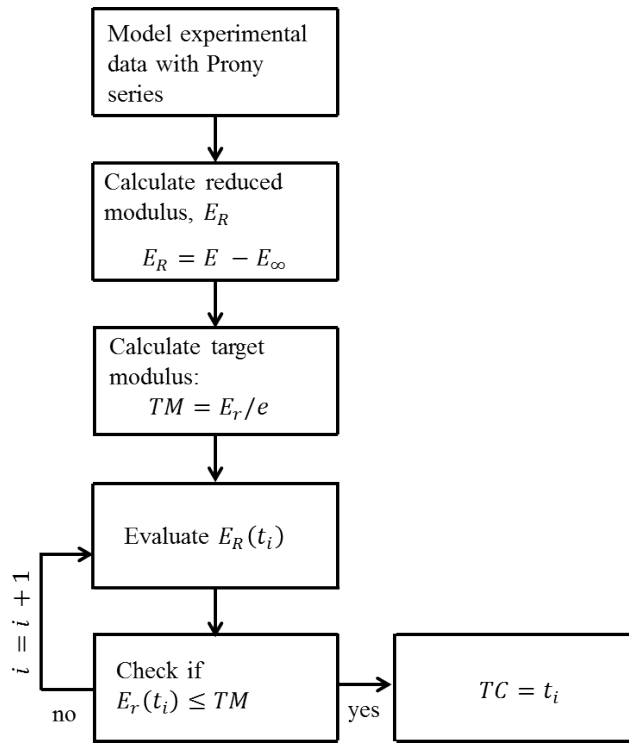

Fig. 6: Flowchart depicting the steps taken to locate the time constant

The time constant information is presented in Table 1 for the six cases in saline ($\mu \approx 0.890$ (mPa s) [38]). With one exception (Saline (d)), the time constant is greater for the higher strain tests. Cartilage takes longer to dissipate energy at higher strains, proportional to the initial value of the response. This finding is interesting because higher strains probably occur during periods of high activity. In effect, cartilage has a higher modulus during periods of higher strain, which likely allows for a more fluid joint motion. This finding agrees with the work of June [39]. The implications for biomimetics are similar- in periods of increased activity (strain), a biomimetic material could be designed to respond with additional cushion or load-support.

The frequency domain offers a different analytic tool for analyzing materials. Ultimately, the goal of characterizing a biphasic material is to understand how it responds in dynamic situations, such as during normal operation or overload. The elastic-viscoelastic correspondence principle transfers time-dependent information to the Laplace and frequency domains without loss of generality. In the
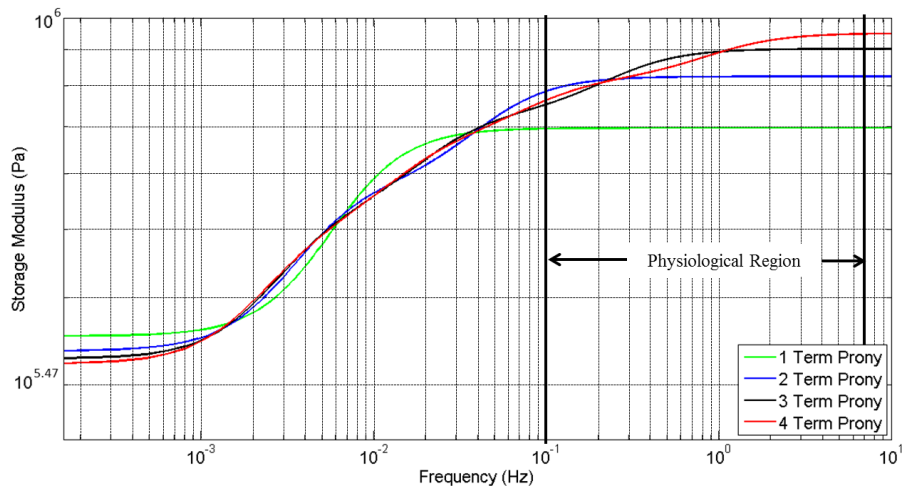
(a) Comparison of the storage information
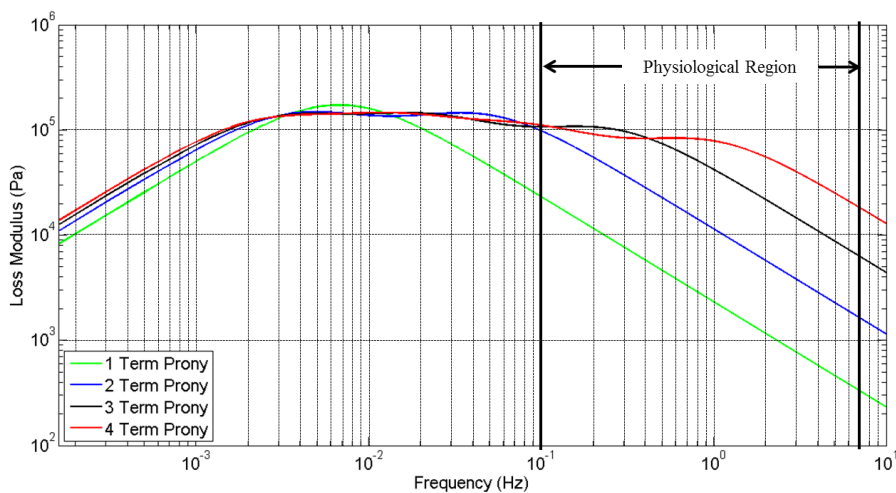
(b) Comparison of the loss information

Fig. 7: Storage and loss comparison of different Prony models (Saline (c))

frequency domain, a stress-relaxation experiment shows the storage and dissipation moduli as a function of frequency, ω. For articular cartilage, the storage and loss moduli are functions of the animal's gait, and for a biomimetic material they are a function of frequency. Studying cartilage as a function of gait offers insight into the adaptive nature of biological mediums. The physiological range of cartilage appears to fall within a transition region, where higher frequencies approach the glassy region and lower frequencies approach the rubbery region. Cartilage can then adjust to a stimulus by storing and dissipating different amounts of energy, depending on the frequency of protuberance. A biomimetic material should have a similar property, dependent on the requirements of the design.

Although an infinite number of Maxwell elements can be used in the Prony series, the problem with using additional terms is threefold: (1) the time-domain curve fitting fails to converge as the number of terms increases, (2) additional terms develop waviness in the frequency domain, and (3) the eigenvalue problem increases in dynamic modeling (as the number of degrees of freedom increases in the model). A comparison of a 1, 2, 3, and 4-term Prony series is presented in Fig. 7(a) for the storage modulus, and Fig. 7(b) for the loss modulus. The development of waviness, or ``wiggles,'' is a construct of the model, *not* a material property. Additionally, the wiggles only appear with significance in the loss modulus.

A trade-off exists between better fitting in the time-domain, and wiggles in the frequency domain. The one and two-term Prony models do not satisfactorily model the rapid decay characteristics of

cartilage during stress-relaxation, and are unable to fully capture the material behavior in the frequency domain. These models are disregarded for that reason. However, the increase in fidelity of the four-term model over the three-term model is relatively minor when considering the norm values of the fits. For a given material, a judgment is made considering the best combination of fitting in the time and frequency domains.

With biological tissues, large variations are expected between samples. It is not surprising since each cartilage explant is unique. Genetics, weight, age, diet, gender, and use can influence the mechanical properties of cartilage. Therefore, the model parameters obtained from experiments are expected to have large variations. This variability is not seen in manufactured substances. One trend that appears ubiquitously is that the transition period of cartilage coincides with the physiological range of exercise. At lower frequencies, cartilage dissipates more energy than at higher frequencies, where additional elasticity is available in the joints. The transition range of cartilage occurs in the middle of the common frequencies of motion (0.25 - 4 Hz). It is possible that the adaptive nature of cartilage is biologically designed for this purpose. The adaptive traits of cartilage could be exploited for a biomimetic material.

One challenge in determining the glassy and rubbery moduli of cartilage is the thickness of the samples is not known *a priori*. The testing procedure imposes a predetermined displacement on the cartilage sample. The strain is determined by the thickness of the sample. Therefore, results obtained from the relaxation experiments are inherently over a range of strains. Attempts were made to limit the strains to 5-15%; however, there are a few cases where 15% is exceeded. Figure 8(a) shows the glassy modulus for the saline cases. Taken together, the six cases seen in Fig. 8(a) do not display a correlation between strain and the instantaneous modulus. Of course, the individual samples typically have a larger glassy moduli at higher strains; however, a general trend for cartilage is not substantiated. The average glassy modulus is obtained by combining all of the samples, and statistical bounds are determined with a Student's t test. This information is presented in Table 2. It should be reiterated that such variations should not be apparent in engineered materials.

On a smaller scale, the rubbery modulus mimics the behavior of the glassy modulus, as shown in Fig. 8(b). The two cases that show higher moduli in the rubbery data also correspond to higher moduli in the glassy data. Neither sample had known physiological differences from the others in the group. A very weak positive correlation ($R^2 = 0.112$) exists between the strain and rubbery moduli information. It is expected that the glassy and rubbery moduli will increase (on average) with higher strains. Physiological limits may dictate if the increase is pronounced or not. The combined rubbery modulus information is included in Table 2.

Both metrics relating to the time constant show no strain dependency for the combined cases. The time constant, found numerically from the four-term Prony series, has no distinguishable trend when considering the samples in saline, as shown in Fig. 8(c). For a given sample, the time constant typically increases with higher strain. The lines linking individual samples together show this phenomenon. One exception exists for both cases. In Table 2, each metric is averaged, and the 95% confidence intervals are given. The absence of a strong trend indicates that cartilage is unique between samples. A generalization of all samples is difficult for this reason. The strain-dependent increase in modulus and time constant seen in most of the individual samples does not appear in the compiled data. In a particular sample, function, weight, age, and other physiological variables likely influence the cartilage response more than strain. The combined results represent a range of likely cartilage behavior, and each sample is said to have certain strain-dependent properties. More exhaustive testing and additional data should be used to corroborate this finding. Regardless, the model and results can serve as a guide for the design of bio-inspired materials.
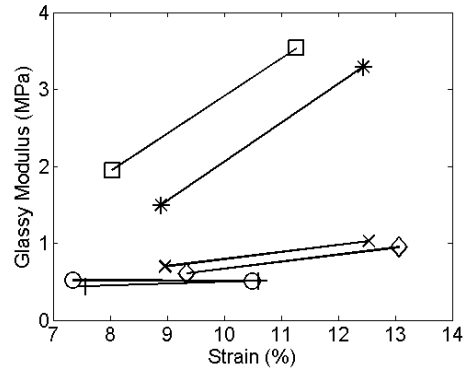
(a) Glassy modulus
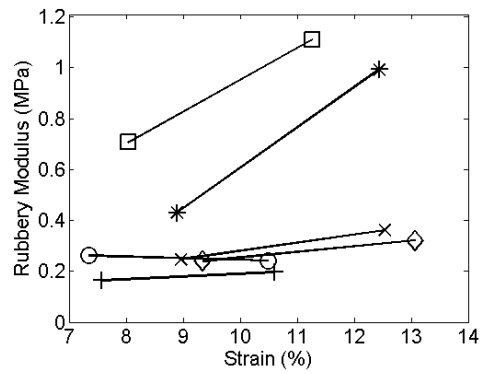
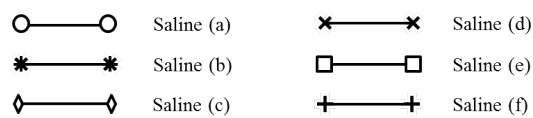(b) Rubbery modulus

(c) Time constant

◯——◯	Saline (a)	✳——✳	Saline (d)
✳——✳	Saline (b)	▢——▢	Saline (e)
◇——◇	Saline (c)	+——+	Saline (f)
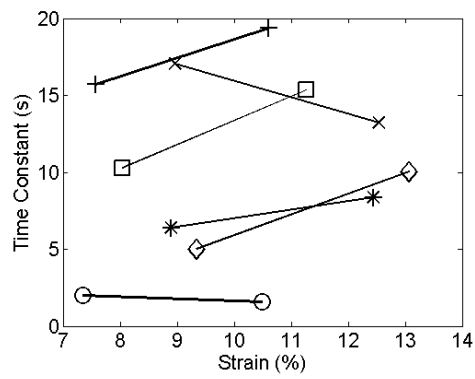
Fig. 8: Results of stress relaxation experiments in saline

Table 2: Tabulated data for saline cases

Fluid Bath	Saline		
Number of Samples	12		
Degrees of Freedom	11		
Strain Range	7.35-13.08%		
	Glassy Modulus [MPa]	Rubbery Modulus [MPa]	Time Constant [s]
Avg.	**1.294**	**0.439**	**10.36**
Std.	1.088	0.321	5.91
SE	0.314	0.093	1.71
Two-Tailed, 95% Student's t test	2.201		
Confidence Interval +/-	0.692	0.204	3.755
Lower Mean	**0.603**	**0.235**	**6.61**
Upper Mean	**1.986**	**0.643**	**14.12**

Discussion

The current study provides a functional alternative to biphasic models for cartilage. The proposed model also has utility in the field of biomimetics. A significant number of additional tests are required to quantitatively describe the behavior of equine cartilage in the stifle joint in general. Limitations of the spring and dashpot models will arise; however, there are many applications where these models are useful. This is particularly apparent in impact studies, and when a multiphase material is used as a component of a larger system.

The experimental data taken from cartilage explants indicates a few interesting trends for biomimetic materials: 1) the bulk mechanical response of a biphasic material like articular cartilage to a fixed displacement can be described with spring and damper systems, 2) cartilage exhibits a correlation between modulus and strain in individual samples; however, the strain-dependency is lost when multiple samples are combined, and 3) in the individual saline cases, with one exception, the time constant increases with strain. These trends are potentially useful in the design of bio-inspired materials.

The current work is focused on providing a model for the stress-relaxation behavior of a biphasic material in unconfined compression. Many previous researchers have used stress-relaxation to determine properties for modeling, but a strictly phenomenological model has not been throughly explored. The majority of tests being performed are creep tests, which are typically easier to execute. However, stress-relaxation experiments are more analogous to movements experienced during exercise. The methods used herein are advantageous compared to previous studies because they more closely mimic biological function, and require fewer material properties. This is a critical point for the modeling of bio-inspired materials.

The transition range of cartilage from a rubbery to glassy modulus is directly in the physiological range of the typical gaits that humans and horses experience. Cartilage is likely either inherently designed to operate in this manner, or it adapts to the user. In either case, this is another unique aspect of cartilage that helps to protect joints and facilitate motion. The tailored nature of cartilage makes it difficult to draw comparisons between samples; however, a general range for the instantaneous modulus is between 0.603 and 1.986 MPa for all of the samples combined. For the equilibrium modulus, the range is between 0.235 and 0.643 MPa. The time constant is: 10.36 s +/- 3.76 s. The strain varied in the tests from 7.3% to 17.9%. A limitation to the current study is the availability of sample explants.

Unconfined compression tests characterize cartilage and similar materials with as few as two types of terms. Poisson's ratio and other experimental ``fudge-factors'' are not required for fitting the data. With a complex material, models that can capture the majority of the mechanical response with relatively few parameters are very useful. Although the relaxation appears to be strain-dependent, the

variation due to strain could be small enough to negate. In addition, biomimetic materials could potentially be designed as strain-independent. The advantage of the phenomenological characterization is its simplicity. The techniques given can be used for comparisons between species, or between healthy and diseased cartilage. The material properties given are needed for a full dynamic or impact study. As discussed, a phenomenological approach is not a mathematical construct of a biphasic material, but it does provide the properties needed for further analysis.

References

[1] Grybos GR (1991) The dynamics of a viscoelastic rotor in flexible bearings. Archive of Applied Mechanics 61(1):479--487

[2] Friswell M (2007) The response of rotating machines on viscoelastic supports. International Review of Mechanical Engineering 1(1):32--40

[3] Elsharkawy AA, Nassar MM (1996) Hydrodynamic lubrication of squeeze-film porous bearings. Acta Mechanica 118:121--134

[4] Charnley J (1960) The lubrication of animal joints in relation to surgical reconstruction by arthroplasty. Annals of the rheumatic diseases 19:10--9

[5] McCutchen CW (1962) The frictional properties of animal joints. Wear 5(1):1--17

[6] Ateshian GA (2009) The role of interstitial fluid pressurization in articular cartilage lubrication. J Biomech 42(9):1163--76

[7] Ateshian GA, Warden WH, Kim JJ, Grelsamer RP, Mow VC (1997) Finite deformation biphasic material properties of bovine articular cartilage from confined compression experiments. Journal of Biomechanics 30(11-12):1157--1164

[8] Ateshian GA, Wang H, Lai WM (1998) The role of interstitial fluid pressurization and surface porosities on the boundary friction of articular cartilage. Journal of Tribology 120(2):241--248

[9] Mow VC, Kuei SC, Lai WM, Armstrong CG (1980) Biphasic creep and stress relaxation of articular cartilage in compression: Theory and experiments. Journal of Biomechanical Engineering 102(1):73--84

[10] Lai WM, Mow VC, Roth V (1981) Effects of nonlinear strain-dependent permeability and rate of compression on the stress behavior of articular cartilage. Journal of Biomechanical Engineering 103(2):61--66

[11] Armstrong CG, Lai WM, Mow VC (1984) An analysis of the unconfined compression of articular cartilage. Journal of Biomechanical Engineering 106(2):165--173

[12] Lai WM, Hou JS, Mow VC (1991) A triphasic theory for the swelling and deformation behaviors of articular cartilage. J Biomech Eng 113(3):245--58

[13] Mow VC, Ateshian GA, Spilker RL (1993) Biomechanics of diarthrodial joints: a review of twenty years of progress. Journal of Biomechanical Engineering 115(4B):460--7

[14] Mow V, Gu W, Chen F (2005) Basic Orthopaedic Biomechanics & Mechano-biology, 3rd edn, Lippincott Williams & Wilkins, Philadelphia, PA, chap Structure and function of articular cartilage and meniscus, pp 181--258

[15] Coletti JM, Akeson WH, Woo SLY (1972) A comparison of the physical behavior of normal articular cartilage and the arthroplasty surface. The Journal of Bone and Joint Surgery 54-A(1):147--160

[16] Parsons JR, Black J (1977) The viscoelastic shear behavior of normal rabbit articular cartilage. Journal of Biomechanics 10(1):21--29

[17] Mak AF (1986) The apparent viscoelastic behavior of articular cartilage---the contributions from the intrinsic matrix viscoelasticity and interstitial fluid flows. Journal of Biomechanical Engineering 108(2):123--130

[18] Woo SLY, Simon BR, Kuei SC, Akeson WH (1980) Quasi-linear viscoelastic properties of normal articular cartilage. Journal of Biomechanical Engineering 102(2):85--90

[19] Fung YC (1967) Elasticity of soft tissues in simple elongation. Am J Physiol 213(6):1532--44

[20] Mow VC, Lipshitz H, Glimcher MJ (1977) Mechanisms for stress relaxation in articular cartilage. In: Society TOR (ed) 23rd Annual Meeting of The Orthopaedic Research Society, The Orthopaedic Research Society, Las Vegas, Nevada, vol 2, p 71

[21] Simon BR, Coats RS, Woo SLY (1984) Relaxation and creep quasilinear viscoelastic models for normal articular cartilage. Journal of Biomechanical Engineering 106(2):159--164

[22] Wang JL, Parnianpour M, ShiraziAdl A, Engin AE (1997) Failure criterion of collagen fiber: Viscoelastic behavior simulated by using load control data. Theoretical and Applied Fracture Mechanics 27(1):1--12

[23] Ehlers W, Markert B (2000) A linear viscoelastic two-phase model for soft tissues.: Application to articular cartilage. ZAMM - Journal of Applied Mathematics and Mechanics / Zeitschrift für Angewandte Mathematik und Mechanik 80(S1):149--152

[24] Ehlers W, Markert B (2001) A linear viscoelastic biphasic model for soft tissues based on the theory of porous media. Journal of Biomechanical Engineering 123(5):418--424

[25] Wilson W, van Donkelaar CC, van Rietbergen B, Ito K, Huiskes R (2004) Stresses in the local collagen network of articular cartilage: a poroviscoelastic fibril-reinforced finite element study. Journal of Biomechanics 37(3):357--366

[26] Wilson W, van Donkelaar CC, van Rietbergen B, Huiskes R (2005) A fibril-reinforced poroviscoelastic swelling model for articular cartilage. Journal of Biomechanics 38(6):1195--1204

[27] DiSilvestro MR, Suh JKF (2001) A cross-validation of the biphasic poroviscoelastic model of articular cartilage in unconfined compression, indentation, and confined compression. Journal of Biomechanics 34(4):519--525

[28] Garcia JJ, Cortes DH (2006) A nonlinear biphasic viscohyperelastic model for articular cartilage. Journal of Biomechanics 39(16):2991--8

[29] Julkunen P, Wilson W, Jurvelin JS, Rieppo J, Qu CJ, Lammi MJ, Korhonen RK (2008) Stress relaxation of human patellar articular cartilage in unconfined compression: Prediction of mechanical response by tissue composition and structure. Journal of Biomechanics 41(9):1978--1986

[30] Argatov II (2013) Mathematical modeling of linear viscoelastic impact: Application to drop impact testing of articular cartilage. Tribology International 63:213--225

[31] Eisenfeld J, Mow VC, Lipshitz H (1978) Mathematical analysis of stress relaxation in articular cartilage during compression. Mathematical Biosciences 39(1-2):97--112

[32] Mow VC, Mansour JM (1977) The nonlinear interaction between cartilage deformation and interstitial fluid flow. Journal of Biomechanics 10(1):31--39

[33] Desai CS, Abel JF (1972) Introduction to the Finite Element Method. Van Nostrand Reinhold Company

[34] Malda J, Benders KEM, Klein TJ, de Grauw JC, Kik MJL, Hutmacher DW, Saris DBF, van Weeren PR, Dhert WJA (2012) Comparative study of depth-dependent characteristics of equine and human osteochondral tissue from the medial and lateral femoral condyles. Osteoarthritis and Cartilage 20(10):1147--1151

[35] Gurtin ME, Sternberg E (1962) On the linear theory of viscoelasticity. Archive for Rational Mechanics and Analysis 11(1):291--356

[36] Szumski RG, Green I (1991) Constitutive laws in time and frequency domains for linear viscoelastic materials. J Acoustical Soc of America 90(40):2292

[37] Miller B, Green I (1997) On the stability of gas lubricated triboelements using the step jump method. Journal of Tribology-Transactions of the Asme 119(1):193--199

[38] Kestin J, Sokolov M, Wakeham WA (1978) Viscosity of liquid water in the range -8 c to 150 c. JPhys Chem Ref Data 7(3):941--948

[39] June RK, Ly S, Fyhrie DP (2009a) Cartilage stress-relaxation proceeds slower at higher compressive strains. Archives of Biochemistry and Biophysics 483(1):75--80